

Superconducting Gravity Gradiometers (SGGs)

Three models of SGGs with increasing complexity and sensitivity have been developed at Maryland [Chan *et al.*, 1987; Moody *et al.*, 2002]. The Model II SGG has reached an operating sensitivity of $0.02 \text{ E Hz}^{-1/2}$ ($1 \text{ E} \equiv 1 \text{ Eötvös} \equiv 10^{-9} \text{ s}^{-2}$), three orders of magnitude improvement over the sensitivity achieved by room-temperature gradiometers. With such vastly improved sensitivity, the SGG finds useful application in geophysical measurements, oil and mineral prospecting, and inertial navigation. The great potential for practical application has inspired several groups around the world to develop similar instruments. At Maryland, a new SGG with improved linear acceleration rejection capability is under development.

Basic Superconducting Accelerometer

Figure 1 shows a superconducting accelerometer in its simplest form. The accelerometer consists of a superconducting proof mass, a superconducting sensing coil and a SQUID with input coil. A persistent current is stored in the loop formed by the sensing coil and the SQUID input coil. When the platform undergoes an acceleration, or equivalently, when a gravity signal is applied, the proof mass is displaced relative to the sensing coil, modulating its inductance through the Meissner effect. This induces a time-varying current in the loop to preserve flux quantization. The SQUID converts the induced current into an output voltage signal.

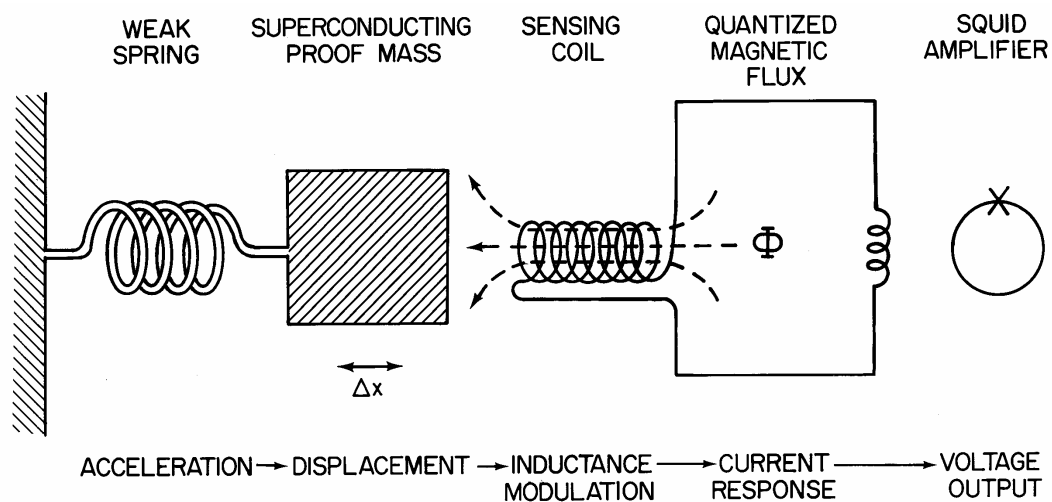


Figure 1. Principle of a superconducting accelerometer.

In-line-Component SGG

Figure 2 shows a component accelerometer of Model II SGG. The proof mass weighing 1.2 kg is suspended by a pair of diaphragm flexures with folded cantilevers. The entire structure is machined from niobium (Nb). Six identical accelerometers are mounted on six faces of a precision titanium (Ti) alloy cube, with the sensitive axes normal to the cube surfaces, to form a three-axis SGG (see Figure 3).

Figure 4 is a schematic circuit diagram for each axis of the Model II SGG. The two proof masses on opposite faces of the mounting cube are connected by a superconducting circuit to form a gradiometer. The proof masses are levitated against gravity by storing a persistent current I_L in the loop formed by L_{L1} and L_{L2} .

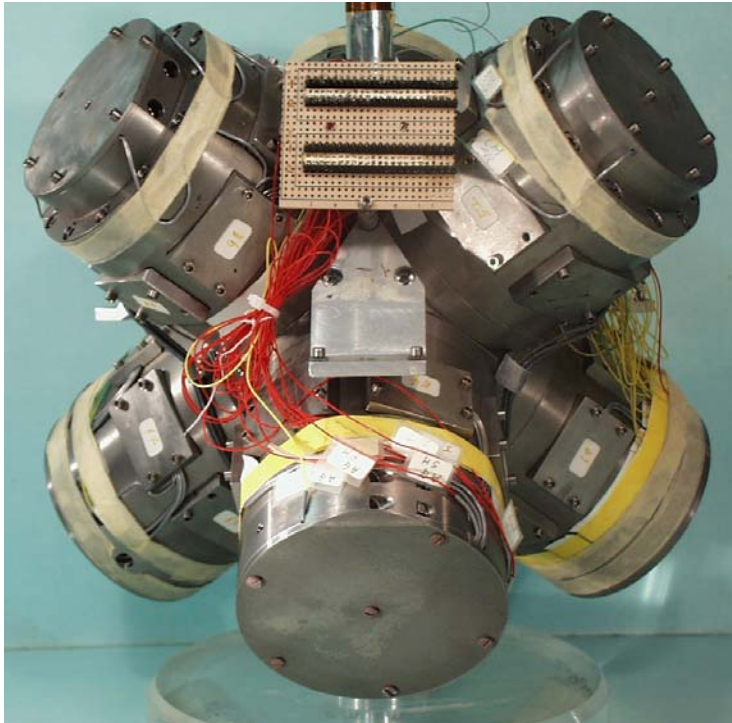


Figure 3. Three-axis Model II SGG.

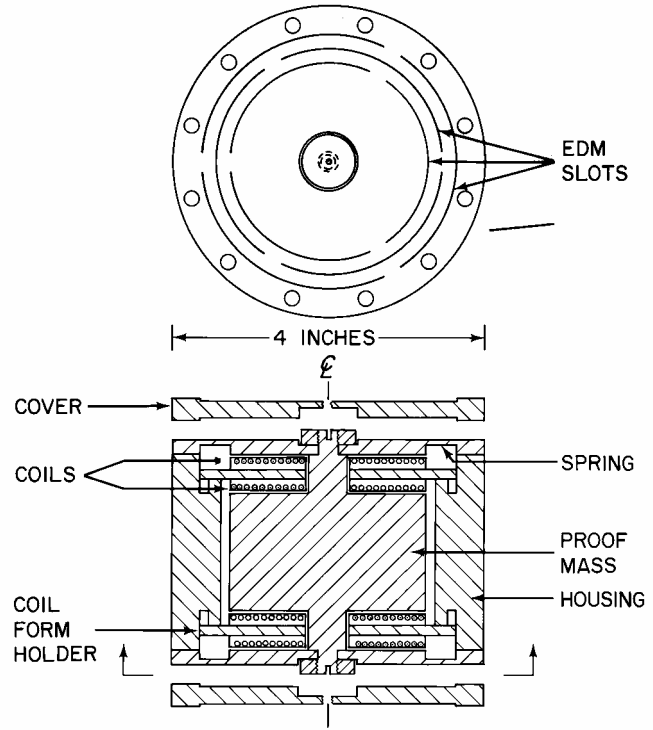


Figure 2. Component accelerometer for Model II SGG.

The proof masses are levitated against gravity by storing a persistent current I_L in the loop formed by L_{L1} and L_{L2} .

The coils L_{S1} and L_{S2} are connected in parallel to a SQUID to form a sensing circuit. Each axis of the gradiometer has two circuits. In one circuit, we store the currents I_{S1} and I_{S2} with the same sense (as shown in Figure 4) and the SQUID detects the differential acceleration, or the gravity gradient. In the other circuit (not shown), we reverse the

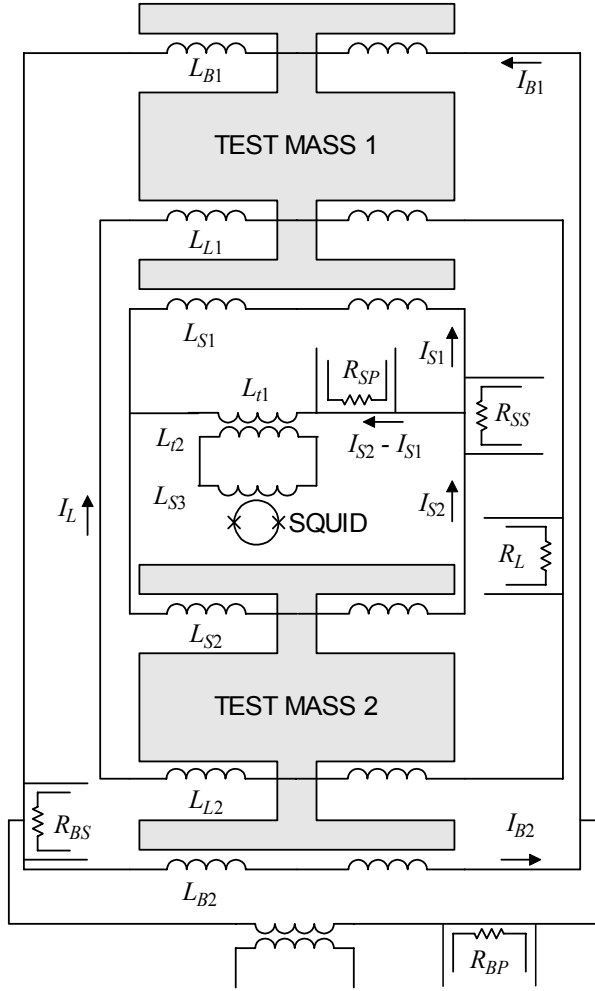


Figure 4. Circuit diagram for each axis of Model II SGG

direction of one of the currents, and the SQUID detects the common-mode motion. Signal differencing by means of persistent currents *before* detection assures excellent null stability of the device, which in turn improves the overall common-mode rejection. Further, the SQUID sees only a small differential signal, thereby reducing the dynamic-range requirement on the amplifier and signal-processing electronics.

We adjust I_{S2}/I_{S1} to maximize the common-mode rejection. Although the component of the linear acceleration parallel to the sensitive axis can be rejected precisely by this current adjustment, components normal to the sensitive axis couple to the gradient output through misalignments of the sensitive axes. In the Model II SGG, all the misalignment angles are measured from the response of the gradiometer to accelerations applied in various directions. The results

are then multiplied by the measured linear acceleration components and subtracted from the gradiometer outputs to achieve the “residual common-mode balance” [Moody *et al.*, 1986]. The misalignments were about 10^{-4} rad. The residual balance improved the common-mode rejection to 10^7 .

The power spectral density of the intrinsic gradient noise of the SGG can be shown to be [Chan and Paik, 1987]

$$S_{\Gamma}(f) = \frac{8}{m\ell^2} \left[k_B T \frac{\omega_0}{Q} + \frac{\omega_0^2}{2\beta\eta} E_A(f) \right], \quad (1)$$

where m , Q and T are the mass, quality factor and temperature of the proof mass, ℓ is the baseline of the gradiometer, β is the electromechanical

energy coupling constant of the transducer, η is the energy coupling efficiency from the superconducting circuit to the SQUID, $E_A(f)$ is the input energy resolution of the SQUID, and $f = \omega/2\pi$ is the signal frequency. The numerical values of the gradiometer parameters are: $m = 1.2$ kg, $\ell = 0.19$ m, $\omega_0/2\pi = 10$ Hz, $Q = 10^6$, $T = 4.2$ K, $\beta = \eta = 0.25$, $E_A(f) = [1 + (0.1 \text{ Hz})/f] 5 \times 10^{-31} \text{ J Hz}^{-1}$ below $f \leq 0.1$ Hz (commercial dc SQUID). Equation (1) predicts a white-noise level of $2 \times 10^{-3} \text{ E Hz}^{-1/2}$. Below 0.1 Hz, a $1/f$ power noise should appear.

Figure 5 shows the actual noise spectrum of the Model II SGG obtained in the laboratory. The white-noise level corresponds to $0.02 \text{ E Hz}^{-1/2}$, dominated by uncompensated angular acceleration noise. Below 0.1 Hz, a $1/f$ power noise appears, but with an amplitude an order of magnitude higher than expected from the SQUID noise. This excess low-frequency noise is believed to come from a combination of temperature drift of the

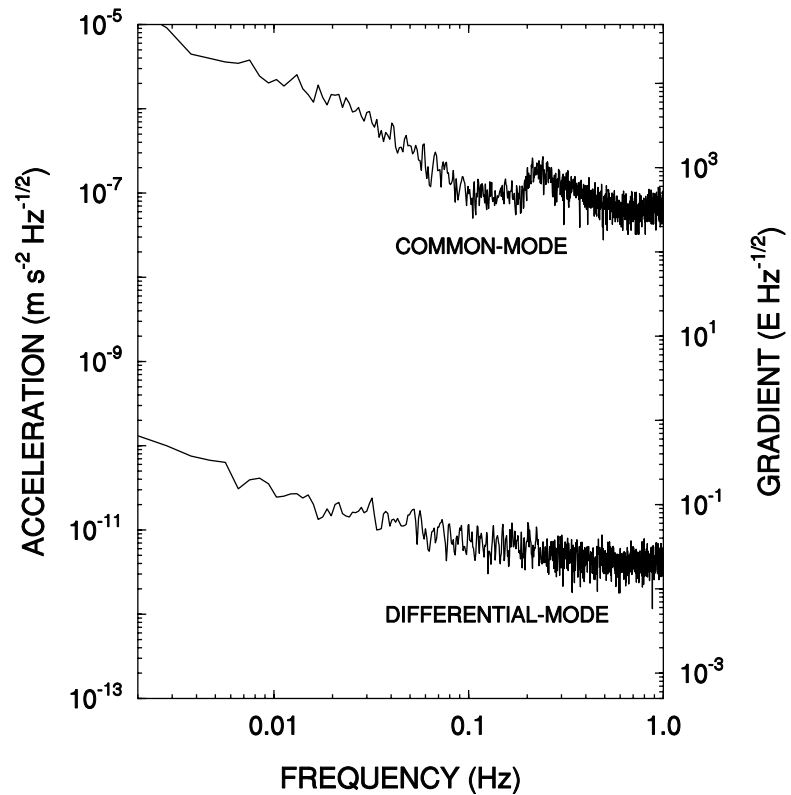


Figure 5. Noise spectrum of Model II SGG.

instrument, which couples to the gradiometer through modulation of the penetration depth of the superconductor, and down-converted centrifugal acceleration noise. The demonstrated sensitivity of the SGG represents three orders of magnitude improvement over that of the conventional gravity gradiometers operated at room temperature.

The sensitivity requirement of NASA's gravity mapping mission have prompted further innovations in technology, a "superconducting negative spring" [Parke *et al.*, 1984]. This has led to the design of the Model III SGG with an intrinsic sensitivity of $10^{-4} \text{ E Hz}^{-1/2}$.

Cross-Component SGG

The in-line-component SGGs have been developed primarily for space application. The achieved common-mode rejection of 10^7 is sufficient for a spacecraft environment. However, for airborne application, the linear acceleration rejection must be improved to 10^9 or higher because the SGG platform cannot be stabilized against the large translational motion experienced by aircraft, which may exceed the dimension of the cabin.

A cross-component gradiometer can be designed to be inherently insensitive to linear accelerations by employing pivoted rotating arms whose mass moments are precisely balanced prior to assembly. Linear accelerations are further discriminated by designing the pivot to be compliant only for the desired rotational acceleration, but stiff against the other degrees of freedom.

Figure 6 shows the three-axis cross-component SGG which is under development at Maryland. The proof mass/pivot structure is cut from a single block of Nb by wire EDM. Two component angular accelerometers on opposite faces of the mounting cube, with their rotating arms oriented orthogonal to each other, are connected together to form a single-axis SGG. Two superconducting circuits, similar to the one shown in Figure 4, are provided to detect the differential (cross-component gradient) and the common-mode (angular acceleration) signals. The expected intrinsic noise of the instrument is $0.02 \text{ E Hz}^{-1/2}$, with a $1/f$ power noise below 0.1 Hz.

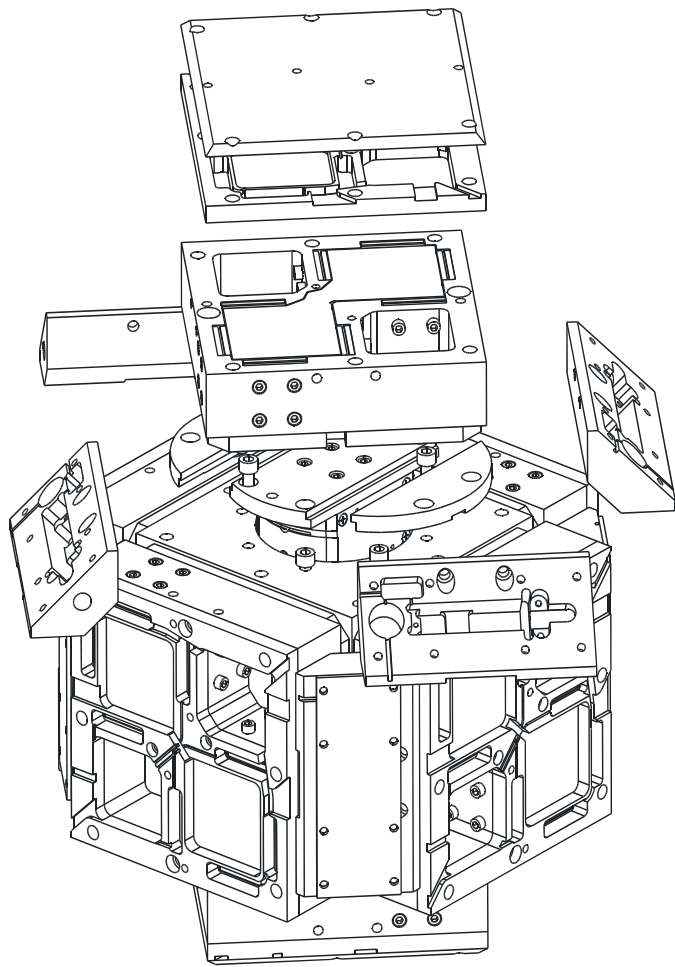


Figure 6. Exploded view of a cross-component SGG.

To eliminate the need for liquid helium, the cross-component SGG is integrated with a dual-stage pulse-tube closed-cycle refrigerator. Figure 7 shows the SGG support structure that is being constructed for laboratory tests of the instrument. The SGG is housed in a vacuum can and supported with a 5-Hz isolation stage to decouple cold head and compressor vibrations. A rigid design eliminates modes near SGG proof mass resonances. The entire structure fits within an envelope 16" diameter and 37" high.

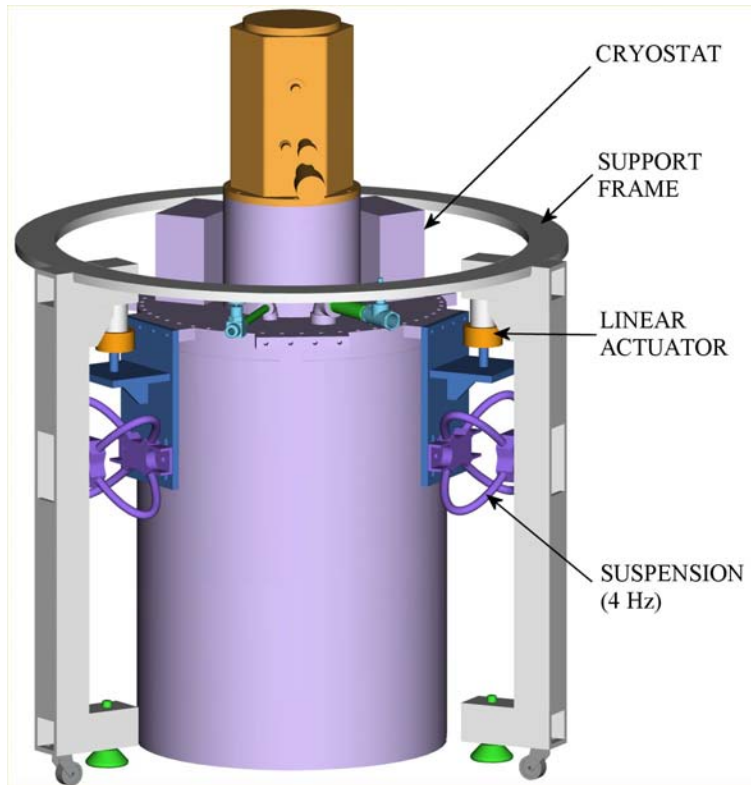


Figure 7. The SGG cryostat on a support structure.

For airborne and shipborne operation, the SGG will be mounted on a stabilized platform. A 40-db attenuation is required to 10 Hz for all three rotation axes.

Chan, H. A. and Paik, H. J. (1987), *Physical Review D* **35**, 3551-3571.
Chan, H. A., Moody, M. V., and Paik, H. J. (1987), *Physical Review D* **35**, 3572-3597.
Moody, M. V., Canavan, E. R., and Paik, H. J. (2002), *Rev. Sci. Instrum.* **73**, 3957.
Moody, M. V., Chan, H. A., and Paik, H. J. (1986), *J. Appl. Phys.* **60**, 4308-4315.
Parke, J. W. *et al.* (1984) in *Proc. 10th International Cryogenic Engineering Conference*, Butterworth, Surrey, D. H. Collan *et al.* (eds.), pp. 361-364.